

SS TRAVELTIME PARAMETERS AND GEOMETRIC SPREADING FROM PP AND PS REFLECTIONS

B. Ursin, M. Tygel and E. Iversen

email: *mtygel@gmail.com*

keywords: *PP, PS, SS, seismic processing, geometrical spreading, amplitudes*

ABSTRACT

Reliable P- and S-wave information is needed for imaging and inversion of seismic data in geologically complex areas. Under current acquisition conditions, shear-wave velocities can only be derived from converted PS-waves included in the data. Because processing of converted waves is much more complicated than for non-converted waves, attempts have been done to use PP- and PS-waves to simulate SS-waves and process these as new data. This has been successfully achieved for the simulation of SS-traveltimes and their slopes and is referred to as the "PP+PS=SS" method. More specifically, the SS-traveltimes and slopes of a target reflector can be obtained from the corresponding PP- and PS-traveltimes and slopes of the same reflector, required that all source and receiver points are located on a common acquisition surface. By using the concept and properties of surface-to-surface propagator matrices, also the second-order traveltimes of the SS-waves are obtained. In fact, the propagator matrix of the SS-wave of a target reflector is explicitly obtained from the propagators of the PP- and PS-wave of the same reflector. Given that the elastic parameters describing S-wave velocities are known along the acquisition surface, this permits to determine the relative geometric spreading of the SS-wave, leading to a better reconstruction of the amplitude of the simulated SS-wave. Under isotropic conditions, the second-order derivatives of the SS-traveltime can, in the same way as for PP-waves, be applied to a tomographic estimation of the S-wave velocity model.

INTRODUCTION

Combined use of P- and S-wave information is widely recognized as crucial for reliable imaging and inversion of seismic data in most situations of reservoir exploration and monitoring interest. Conventional processing of PP waves alone is unable to assess structural properties such as anisotropy, as well as to account to lithology complications, such as gas clouds in reservoir overburden.

In principle, processing of SS waves, if available in the seismic data, would parallel the one routinely carried out for PP waves to provide the corresponding S-wave information. Such a simple and direct procedure is precluded, however, as present-day seismic data, e.g., as acquired using ocean-bottom technology, include PP and PS waves, but not SS waves as reliable energy. In this way, extraction of S-wave seismic parameters has to come from the PS waves in the data.

As described in, e.g., Thomsen (1999), processing of P-to-S converted data poses a number of difficulties, due to its asymmetric traveltime. Namely, as reciprocity of PS is SP (and not PS), traveltime is a function of offset, but not of offset squared, a property Thomsen refers to as "dioidic". As a consequence, the familiar velocity analysis based on the hyperbolic normal-moveout (NMO) traveltimes or their non-hyperbolic extensions do not apply. In spite of several attempts to overcome its difficulties and actually process PS-waves directly from the data (see, e.g., Tessmer and Behle, 1988; Tsvankin and Grechka, 2000), no simple satisfactory procedure has up to now been offered.

To overcome the above-indicated difficulties, Grechka and Tsvankin (2002) introduced a method to (kinematically) simulate SS reflections by means of a suitable combination of PP- and PS-reflections. More

specifically, the method, referred to as “PP+PS=SS” method, selects identified traveltimes and slopes of PP and PS reflections of the same reflector to produce the corresponding SS reflection from that reflector. The sources and receivers of the PP and PS events must be located on a common acquisition surface. Upon the application of such procedure, the obtained SS reflections can be incorporated to the original seismic volume as SS-reflection data. As such, they can, in principle, be processed by velocity-analysis methods designed in the same way as for PP waves.

So far, the “PP+PS=SS” method uses the traveltimes and slopes of the PP and PS waves to provide the corresponding traveltimes and slopes of the simulated SS-reflections. A natural question arises, namely, whether the knowledge of the second-order traveltime derivatives of PP and PS waves, as provided by their ray-propagator matrices, lead to the ray-propagator matrix of the corresponding SS wave. In this paper, we show that the answer of that question is affirmative. By using the “algebra” of ray-propagator matrices, as introduced by Bortfeld (1989) and further developed by Iversen (2006), an explicit relationship between the involved PP-, PS- and SS-ray-propagator matrices is achieved.

By examining the relationships that exist between the coefficients of the second-order Taylor expansion of traveltime (see, e.g., Ursin, 1982) and the submatrix components of the PP, PS and SS ray-propagator matrices, we see that the new results provide the second-order derivatives of SS traveltime, thus extending the counterpart zero- and first-order derivatives provided by the “PP+PS=SS” method. Given in addition that the elastic parameters that determine the S-wave velocities are known along the acquisition surface, this enables the estimation of the relative geometric spreading of the SS wave, the inverse of which constitutes the “geometric amplitude” of that wave.

In the zero-offset situation, the second-order derivatives of non-converted traveltimes, namely PP and SS, yield NMO-velocities or NIP-wave curvatures (Hubral, 1983). In this way, one avoids traveltime processing to obtain these velocities. Together with the traveltimes and slopes, the NIP-wave curvatures can be applied to tomographic inversion in isotropic models for the corresponding P- and S-wave velocity fields (see, e.g., Iversen and Gjøystdal, 1984; Duvencek, 2004). For depth-consistent tomography of PP and PS reflections it is necessary that key reflectors are imaged at the same depth. Foss et al. (2005) used the zero-offset PP and PS traveltimes to estimate the SS reflection times. These were then used together with the PP traveltimes for reflector co-dephing.

We finally observe that a full simulation of the SS wave, which should include the reflection and transmission coefficients, is not possible. In fact, the SS reflection/transmission coefficients cannot be determined from the amplitudes of PP- and PS-reflected waves. For a better assessment on the reflection/transmission coefficients expressions for the various wavemodes PP, PS and SS, the reader is referred to Chapman (1994) and Stovas and Ursin (2003).

TAYLOR SERIES TRAVELTIME APPROXIMATIONS

We consider a group of sources located at $\mathbf{x}^s + \Delta\mathbf{x}^s$ near a central source point \mathbf{x}^s and a group of receivers located at $\mathbf{x}^r + \Delta\mathbf{x}^r$ near a central receiver point \mathbf{x}^r . For a multiple transmitted and reflected wave the traveltime may be expanded in a Taylor series series (Ursin, 1982; Červený et al., 1984)

$$T(\mathbf{x}^r + \Delta\mathbf{x}^r, \mathbf{x}^s + \Delta\mathbf{x}^s) = T(\mathbf{x}^r, \mathbf{x}^s) + (\mathbf{p}^r)^T \Delta\mathbf{x}^r - (\mathbf{p}^s)^T \Delta\mathbf{x}^s + (\Delta\mathbf{x}^r)^T \mathbf{M}^{rs} \Delta\mathbf{x}^s + \frac{1}{2} (\Delta\mathbf{x}^r)^T \mathbf{M}^{rr} \Delta\mathbf{x}^r + \frac{1}{2} (\Delta\mathbf{x}^s)^T \mathbf{M}^{ss} \Delta\mathbf{x}^s. \quad (1)$$

Here, all vectors are column vectors of size three, and superscript T denotes transpose. Also, \mathbf{p}^r and \mathbf{p}^s denote the slowness vectors at \mathbf{x}^r and \mathbf{x}^s , respectively, and the 3×3 matrices \mathbf{M}^{rr} , \mathbf{M}^{rs} and \mathbf{M}^{ss} contain the second-order derivatives of traveltime with respect to \mathbf{x}^r and \mathbf{x}^s as denoted in the superscript. The symmetric matrix \mathbf{M}^{rr} is related to the wavefront curvatures at \mathbf{x}^r for a source at \mathbf{x}^s , while the symmetric matrix \mathbf{M}^{ss} is related to the wavefront curvatures at \mathbf{x}^s for a source at \mathbf{x}^r . The matrix \mathbf{M}^{rs} of second-order mixed derivatives is related to the relative geometric spreading, see the Appendix A.

By squaring equation 1 and retaining the terms up to second order only, we obtain the more commonly used Taylor series for traveltime squared

$$T(\mathbf{x}^r + \Delta\mathbf{x}^r, \mathbf{x}^s + \Delta\mathbf{x}^s)^2 = [T(\mathbf{x}^r, \mathbf{x}^s) + (\mathbf{p}^r)^T \Delta\mathbf{x}^r - (\mathbf{p}^s)^T \Delta\mathbf{x}^s]^2 + T(\mathbf{x}^r, \mathbf{x}^s)[2(\Delta\mathbf{x}^r)^T \mathbf{M}^{rs} \Delta\mathbf{x}^s + (\Delta\mathbf{x}^r)^T \mathbf{M}^{rr} \Delta\mathbf{x}^r + (\Delta\mathbf{x}^s)^T \mathbf{M}^{ss} \Delta\mathbf{x}^s]. \quad (2)$$

We shall assume that all sources and receivers are located on a common acquisition surface. For simplicity, we let this surface be the plane $x_3 = 0$. As a consequence, we will in the following consider the vectors and matrices in equations 1 and 2 to have dimensions two and 2×2 , respectively. The traveltimes approximations in equations 1 and 2 are valid for a single traveltime branch in a heterogeneous anisotropic medium. As shown in numerical examples by Gjøystdal et al. (1984), there are cases where equation 1 is more accurate than equation 2 and other cases where the opposite is true. The range of validity of these equations may, however, be very small or even non-existent. This was shown by Tygel et al. (2007) for qSV reflections in a horizontally layered VTI medium (transversely isotropic medium with a vertical symmetry axis). In this case there can be a traveltime triPLICATION on the vertical axis, which strongly limits the range of validity of the power series expansion. In the following, we shall assume that the traveltime Taylor series expansions are valid, and that the traveltime parameters, $T(\mathbf{x}^r, \mathbf{x}^s)$, \mathbf{p}^r , \mathbf{p}^s , \mathbf{M}^{rr} , \mathbf{M}^{rs} and \mathbf{M}^{ss} , can be estimated from the seismic data.

In the following derivations, we shall use the 4×4 surface-to-surface ray propagator matrix (Bortfeld, 1989; Iversen, 2006)

$$\Sigma(\mathbf{x}^r, \mathbf{x}^s) = \begin{pmatrix} \mathbf{A} & \mathbf{B} \\ \mathbf{C} & \mathbf{D} \end{pmatrix}, \quad (3)$$

where \mathbf{A} , \mathbf{B} , \mathbf{C} , and \mathbf{D} are 2×2 constant submatrices, which incorporate the dynamic quantities (second-order derivatives of traveltime) of the central ray, as well as the properties of the anterior surface (where the central ray starts) and the posterior surface (where the central ray emerges). The submatrix elements of the surface-to-surface propagator matrix satisfy the following relationships:

$$[\Sigma(\mathbf{x}^r, \mathbf{x}^s)]^{-1} = \begin{pmatrix} \mathbf{D}^T & -\mathbf{B}^T \\ -\mathbf{C}^T & \mathbf{A}^T \end{pmatrix}, \quad (4)$$

and

$$\Sigma(\mathbf{x}^s, \mathbf{x}^r) = [\Sigma(\mathbf{x}^r, \mathbf{x}^s)]^{rev} = \begin{pmatrix} \mathbf{D}^T & \mathbf{B}^T \\ \mathbf{C}^T & \mathbf{A}^T \end{pmatrix}. \quad (5)$$

In equation 5 the operation signified by the superscript *rev* implies that the resulting propagator matrix on the left-hand side corresponds to the reverse ray direction, i.e., the direction from \mathbf{x}^r to \mathbf{x}^s rather than from \mathbf{x}^s to \mathbf{x}^r . From equations 3 and 4 we obtain

$$\mathbf{C} = (\mathbf{D}\mathbf{A}^T - \mathbf{I})\mathbf{B}^{-T}, \quad (6)$$

where \mathbf{I} is the 2×2 identity matrix and the superscript $-T$ denotes the transpose of the inverse matrix.

The second-order traveltime derivative matrices are related to the elements of the surface-to-surface ray propagator by the equations (Červený, 2001)

$$\mathbf{M}^{rr} = \mathbf{D}\mathbf{B}^{-1}, \quad \mathbf{M}^{ss} = \mathbf{B}^{-1}\mathbf{A} \quad \text{and} \quad \mathbf{M}^{rs} = -\mathbf{B}^{-1}. \quad (7)$$

From these, we obtain

$$\mathbf{B} = -(\mathbf{M}^{rs})^{-1}, \quad \mathbf{A} = -(\mathbf{M}^{rs})^{-1}\mathbf{M}^{ss}, \quad \text{and} \quad \mathbf{D} = -\mathbf{M}^{rr}(\mathbf{M}^{rs})^{-1}, \quad (8)$$

so that, from equation 6,

$$\mathbf{C} = (\mathbf{M}^{rs})^T - \mathbf{M}^{rr}(\mathbf{M}^{rs})^{-1}\mathbf{M}^{ss}. \quad (9)$$

SS TRAVELTIME PARAMETERS

We consider one PP and two PS reflection waves as shown in Figure 1. The points \mathbf{x}^a , \mathbf{x}^b , \mathbf{x}^c and \mathbf{x}^d lie on the common acquisition surface for sources and receivers, while the slowness vectors and the normal vector, \mathbf{n} , of the reflecting interface at the reflection point, \mathbf{y} , all lie in a common plane (Snell's law). In order to find the points \mathbf{x}^b and \mathbf{x}^c on the acquisition surface, a PP reflection is first identified for the couple $(\mathbf{x}^a, \mathbf{x}^d)$ and its traveltime parameters estimated. Next, the PS waves from \mathbf{x}^a to \mathbf{x}^c and from \mathbf{x}^d to \mathbf{x}^b are identified such that the slowness vectors of the P waves at \mathbf{x}^a and \mathbf{x}^d are parallel to the corresponding

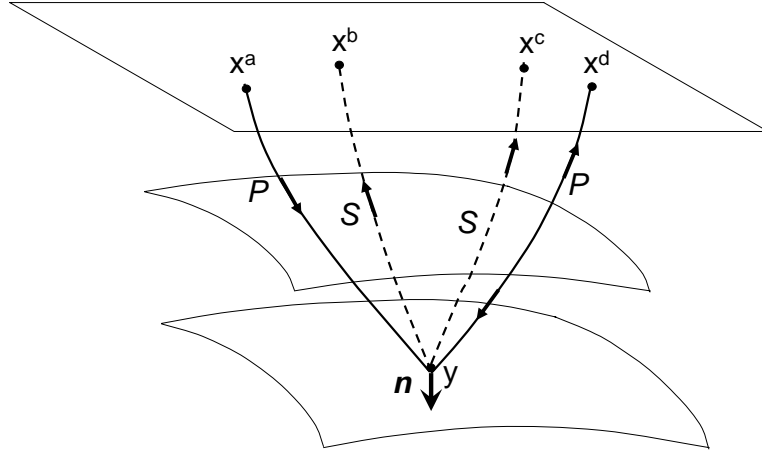


Figure 1: Geometry of a common-offset image gather.

PP-wave slowness vectors at the same points (Grechka et al., 2002; Grechka and Tsvankin, 2002). The traveltime parameters for the two PS waves are also estimated. Then the traveltime for the SS wave is

$$T^{SS}(\mathbf{x}^c, \mathbf{x}^b) = T^{SP}(\mathbf{x}^c, \mathbf{x}^a) + T^{SP}(\mathbf{x}^b, \mathbf{x}^d) - T^{PP}(\mathbf{x}^d, \mathbf{x}^a). \quad (10)$$

Using the multiplicative rule for the surface-to-surface ray propagators, these are given, for the PP and two PS reflections, by

$$\begin{aligned} \Sigma^{PP}(\mathbf{x}^d, \mathbf{x}^a) &= \Sigma^P(\mathbf{x}^d, \mathbf{y})\Sigma^P(\mathbf{y}, \mathbf{x}^a), \\ \Sigma^{SP}(\mathbf{x}^c, \mathbf{x}^a) &= \Sigma^S(\mathbf{x}^c, \mathbf{y})\Sigma^P(\mathbf{y}, \mathbf{x}^a), \\ \Sigma^{SP}(\mathbf{x}^b, \mathbf{x}^d) &= \Sigma^S(\mathbf{x}^b, \mathbf{y})\Sigma^P(\mathbf{y}, \mathbf{x}^d). \end{aligned} \quad (11)$$

Here, the superscript denotes the wavetype and the indexing is from right to left (as in equation 10). For further use, we also note that

$$[\Sigma^{SP}(\mathbf{x}^b, \mathbf{x}^d)]^{rev} = \Sigma^{PS}(\mathbf{x}^d, \mathbf{x}^b) = \Sigma^P(\mathbf{x}^d, \mathbf{y})\Sigma^S(\mathbf{y}, \mathbf{x}^b). \quad (12)$$

It follows that the ray propagator for the SS wave from \mathbf{x}^b to \mathbf{x}^c is given by

$$\Sigma^{SS}(\mathbf{x}^c, \mathbf{x}^b) = \Sigma^{SP}(\mathbf{x}^c, \mathbf{x}^a)[\Sigma^{PP}(\mathbf{x}^d, \mathbf{x}^a)]^{-1}[\Sigma^{SP}(\mathbf{x}^b, \mathbf{x}^d)]^{rev}, \quad (13)$$

where the inverse and reverse matrices are given in equations 4 and 5, respectively. The above important result is seen from

$$\begin{aligned} \Sigma^{SS}(\mathbf{x}^c, \mathbf{x}^b) &= \Sigma^S(\mathbf{x}^c, \mathbf{y})\Sigma^S(\mathbf{y}, \mathbf{x}^b) \\ &= \Sigma^S(\mathbf{x}^c, \mathbf{y}) \left\{ \Sigma^P(\mathbf{y}, \mathbf{x}^a)[\Sigma^P(\mathbf{y}, \mathbf{x}^a)]^{-1} \right\} \left\{ [\Sigma^P(\mathbf{x}^d, \mathbf{y})]^{-1} \Sigma^P(\mathbf{x}^d, \mathbf{y}) \right\} \Sigma^S(\mathbf{y}, \mathbf{x}^b) \\ &= \left\{ \Sigma^S(\mathbf{x}^c, \mathbf{y})\Sigma^P(\mathbf{y}, \mathbf{x}^a) \right\} \left\{ [\Sigma^P(\mathbf{y}, \mathbf{x}^a)]^{-1} [\Sigma^P(\mathbf{x}^d, \mathbf{y})]^{-1} \right\} \left\{ \Sigma^P(\mathbf{x}^d, \mathbf{y})\Sigma^S(\mathbf{y}, \mathbf{x}^b) \right\} \\ &= \left\{ \Sigma^S(\mathbf{x}^c, \mathbf{y})\Sigma^P(\mathbf{y}, \mathbf{x}^a) \right\} \left\{ \Sigma^P(\mathbf{x}^d, \mathbf{y})\Sigma^P(\mathbf{y}, \mathbf{x}^a) \right\}^{-1} \left\{ \Sigma^P(\mathbf{x}^d, \mathbf{y})\Sigma^S(\mathbf{y}, \mathbf{x}^b) \right\}. \end{aligned} \quad (14)$$

The desired result 13 now follows from the first two equations 11 and equation 12.

From the surface-to-surface ray propagator matrix for the SS wave, we can compute the second-order traveltime parameters using equation 7.

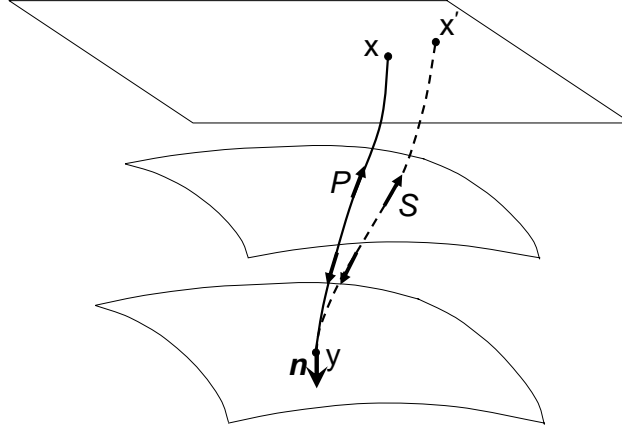


Figure 2: Normal-incidence PP and SS reflections.

NORMAL-INCIDENCE REFLECTIONS

It is common to estimate traveltme parameters in midpoint, half-offset coordinates

$$\mathbf{x}^m = \frac{1}{2}(\mathbf{x}^r + \mathbf{x}^s) \quad \text{and} \quad \mathbf{h} = \frac{1}{2}(\mathbf{x}^r - \mathbf{x}^s). \quad (15)$$

For a normal-incidence ray, which is reflected at an interface so that the slowness vector is parallel to the interface normal, and the ray code up is equal to the ray code down, the source and receiver points coincide. The Taylor series for traveltme then becomes (Ursin, 1982)

$$T(\mathbf{x}^m + \Delta\mathbf{x}^m, \mathbf{h}) = T(\mathbf{x}^m, \mathbf{0}) + (\mathbf{p}^x)^T \Delta\mathbf{x}^m + \frac{1}{2}(\Delta\mathbf{x}^m)^T \mathbf{M}^{xx} \Delta\mathbf{x}^m + \frac{1}{2}\mathbf{h}^T \mathbf{M}^{hh} \mathbf{h}, \quad (16)$$

where the two-component vector \mathbf{p}^x and 2×2 matrix \mathbf{M}^{xx} constitute, respectively, the first- and second-order traveltme derivatives for a given event in the zero-offset data cube, and the 2×2 matrix \mathbf{M}^{hh} defines the NMO velocities (the NMO ellipse, see Grechka and Tsvankin (2002). Traveltme squared is given, always in second-order approximation, by

$$T(\mathbf{x}^m + \Delta\mathbf{x}^m, \mathbf{h})^2 = [T(\mathbf{x}^m, \mathbf{0}) + (\mathbf{p}^x)^T \Delta\mathbf{x}^m]^2 + T(\mathbf{x}^m, \mathbf{0})[(\Delta\mathbf{x}^m)^T \mathbf{M}^{xx} \Delta\mathbf{x}^m + \mathbf{h}^T \mathbf{M}^{hh} \mathbf{h}]. \quad (17)$$

In this case (Ursin, 1982)

$$\mathbf{M}^{rr} = \frac{1}{4}[\mathbf{M}^{xx} + \mathbf{M}^{hh}] = \mathbf{M}^{ss} \quad \text{and} \quad \mathbf{M}^{rs} = \frac{1}{4}[\mathbf{M}^{xx} - \mathbf{M}^{hh}] = [\mathbf{M}^{rs}]^T. \quad (18)$$

For the surface-to-surface ray propagator, we have (Iversen, 2006)

$$\mathbf{A} = \mathbf{D}^T, \quad \mathbf{B} = \mathbf{B}^T \quad \text{and} \quad \mathbf{C} = \mathbf{C}^T. \quad (19)$$

Using equations 8, 9, and 18 and applying some elementary matrix algebra, we obtain

$$\begin{aligned} \mathbf{B} &= 4(\mathbf{M}^{hh} - \mathbf{M}^{xx})^{-1}, \\ \mathbf{A} &= (\mathbf{M}^{hh} - \mathbf{M}^{xx})^{-1}(\mathbf{M}^{hh} + \mathbf{M}^{xx}) = \mathbf{D}^T, \\ \mathbf{C} &= \mathbf{M}^{hh}(\mathbf{M}^{hh} - \mathbf{M}^{xx})^{-1}\mathbf{M}^{xx}. \end{aligned} \quad (20)$$

This also means that matrix \mathbf{C} satisfies the relation

$$\mathbf{C}^{-1} = (\mathbf{M}^{\mathbf{xx}})^{-1} - (\mathbf{M}^{\mathbf{hh}})^{-1}. \quad (21)$$

Figure 2 shows a PP and an SS reflection with the same normal-incidence reflection point, \mathbf{y} . First we identify the normal-incidence reflection at the surface point, \mathbf{x} , and estimate its traveltime parameters. Next we identify the PS reflection with the receiver point at \mathbf{x}' and with the same slopes at the source at \mathbf{x} as the normal-incidence PP reflection. The traveltime parameters for the PS-reflected wave are also estimated. Then the traveltime for the normal-incidence SS reflection is (Foss et al., 2005)

$$T^{SS}(\mathbf{x}') = 2T^{SP}(\mathbf{x}', \mathbf{x}) - T^{PP}(\mathbf{x}). \quad (22)$$

The slope vector for the SS reflection is

$$\mathbf{p}^x(\mathbf{x}') = 2\mathbf{p}^r(\mathbf{x}'), \quad (23)$$

where $\mathbf{p}^r(\mathbf{x}')$ is the corresponding slope vector at the receiver for the PS-reflected wave. The surface-to-surface ray propagator for the normal-incidence SS wave is given by equation 13 with $\mathbf{x}^a = \mathbf{x}^d = \mathbf{x}$ and $\mathbf{x}^b = \mathbf{x}^c = \mathbf{x}'$, namely

$$\Sigma^{SS}(\mathbf{x}', \mathbf{x}') = \Sigma^{SP}(\mathbf{x}', \mathbf{x})[\Sigma^{PP}(\mathbf{x}, \mathbf{x})]^{-1}[\Sigma^{SP}(\mathbf{x}', \mathbf{x})]^{rev}. \quad (24)$$

In equation 24 the surface-to-surface ray propagator for the PS wave must be computed with the general traveltime approximations 1 or 2 and with equation 20. The surface-to-surface ray propagator for the normal-incidence PP wave can be computed from the simplified traveltime approximations 16 or 17 and using equation 20.

SLOPE MATCHING BASED ON SECOND-ORDER TRAVELTIME DERIVATIVES

The extended “PP+PS=SS” method described above makes use of computed second derivatives of PP- and PS-wave traveltimes. This offers the possibility of utilizing such derivatives in the required matching of slopes belonging to the two wavefields.

Consider the problem of finding a root \mathbf{x} of the nonlinear vector equation $\mathbf{f}(\mathbf{x}) = \mathbf{0}$ using an iteration technique of the Newton-Raphson type. The inherent linearization of each iteration step yields the following update of \mathbf{x} with respect to the current solution \mathbf{x}^0 ,

$$\mathbf{x} = \mathbf{x}^0 - \left[\frac{\partial \mathbf{f}}{\partial \mathbf{x}^T}(\mathbf{x}^0) \right]^{-1} \mathbf{f}(\mathbf{x}^0). \quad (25)$$

The slope matching consists of two independent steps, which collectively make use of equation 25. In the first step we consider a PS wave for which the source point is located at \mathbf{x}^a . The function \mathbf{f} then has the definition

$$\mathbf{f}(\mathbf{x}) = \frac{\partial T^{PP}}{\partial \mathbf{x}^a}(\mathbf{x}^d, \mathbf{x}^a) - \frac{\partial T^{SP}}{\partial \mathbf{x}^a}(\mathbf{x}, \mathbf{x}^a), \quad (26)$$

with the first derivatives given by

$$\frac{\partial \mathbf{f}}{\partial \mathbf{x}^T}(\mathbf{x}) = \frac{\partial^2 T^{SP}}{\partial \mathbf{x} \partial \mathbf{x}^a T}(\mathbf{x}, \mathbf{x}^a) = -\mathbf{M}^{rs}(\mathbf{x}, \mathbf{x}^a). \quad (27)$$

The matrix \mathbf{M}^{rs} in equation 27 belongs to the PS wave. In the second step we consider another PS wave, having \mathbf{x}^d as its source point. The function \mathbf{f} and its derivatives can now be specified by

$$\mathbf{f}(\mathbf{x}) = \frac{\partial T^{PP}}{\partial \mathbf{x}^d}(\mathbf{x}^a, \mathbf{x}^d) - \frac{\partial T^{SP}}{\partial \mathbf{x}^d}(\mathbf{x}, \mathbf{x}^d), \quad (28)$$

$$\frac{\partial \mathbf{f}}{\partial \mathbf{x}^T}(\mathbf{x}) = \frac{\partial^2 T^{SP}}{\partial \mathbf{x} \partial \mathbf{x}^d T}(\mathbf{x}, \mathbf{x}^d) = -\mathbf{M}^{rs}(\mathbf{x}, \mathbf{x}^d). \quad (29)$$

Again, the matrix \mathbf{M}^{rs} belongs to the PS wave.

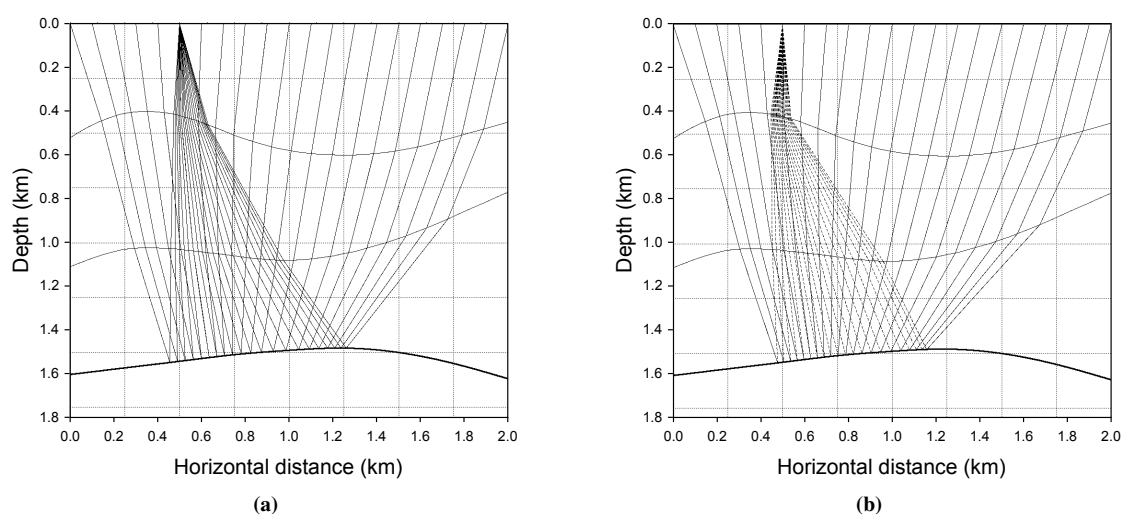


Figure 3: (a) PP-wave rays and (b) PS-wave rays for a common receiver at $x = 0.5$ km in a model similar to the one used by Grechka and Tsvankin (2002)

NUMERICAL EXAMPLE

In this section we present a numerical example demonstrating the extended “PP+PS=SS” method. Our experiment is conducted with a model similar to the one used by Grechka and Tsvankin (2002). The model is two-dimensional and consists of three homogeneous layers containing anisotropy of the VTI type. The layers are separated by smoothly curved interfaces, which were generated by digitizing the interfaces plotted in Grechka and Tsvankin’s (2002) paper. For the latter reason, the models used by Grechka and Tsvankin (2002) and us are not exactly the same; however, for practical purposes they can be considered equal. The waves under consideration in the experiment are of P and SV types; hence, in each layer the wave propagation is described in terms of four parameters, specified using Thomsen (1999) representation:

- Top layer: $V_{P0} = 2.0$ km/s, $V_{S0} = 0.8$ km/s, $\epsilon = 0.20$, $\delta = 0.10$
- Middle layer: $V_{P0} = 2.5$ km/s, $V_{S0} = 1.25$ km/s, $\epsilon = 0.25$, $\delta = 0.05$
- Bottom layer: $V_{P0} = 3.0$ km/s, $V_{S0} = 1.8$ km/s, $\epsilon = 0.15$, $\delta = 0.10$

Traveltime “observations” corresponding to PP and PS reflections from the lower interface of the bottom layer were generated using ray tracing. Figure 3 shows PP rays (a) and PS rays (b) for a common receiver at the horizontal coordinate $x = 0.5$ km. The corresponding traveltime observations for all source and receiver locations are shown, respectively, in Figures 4(a) and 4(b). The simulated “true” traveltimes for the SS reflections are displayed in Figure 4(c). Comparing to Figures 5 and 8 in Grechka and Tsvankin (2002) one finds a convincing consistency between the PP-, PS-, and SS-traveltimes computed using their and our model.

The (a), (b), and (c) subfigures constituting Figure 5 show the PP-, PS-, and SS-wave relative geometric spreading computed using the traveltime data in the corresponding subfigures of Figure 5. The simulated “true” SS-wave relative geometric spreading in Figure 5(c) is used below for comparison with the estimated results obtained using the extended “PP+PS=SS” method. The simulated relative geometric spreading for the PP- and PS-waves [Figures 5(a) and 5(b)] are not used in this method, but the two plots nevertheless serve to indicate the stability of the second-derivatives of the observed PP and PS traveltime functions.

In Figure 6, we have plotted the reconstructed SS-wave source-receiver pairs that form the basis of the estimation of SS-wave traveltimes and relative geometric spreading factors. This plot is to be compared with Figure 6 in Grechka and Tsvankin (2002), and again, one finds very similar results. Figure 7(a) shows the SS-wave traveltimes estimated using the previously published “PP+PS=SS” method, which is to be compared with Figure 4(c). The discrepancy between the two results is displayed in Figure 7(b). We

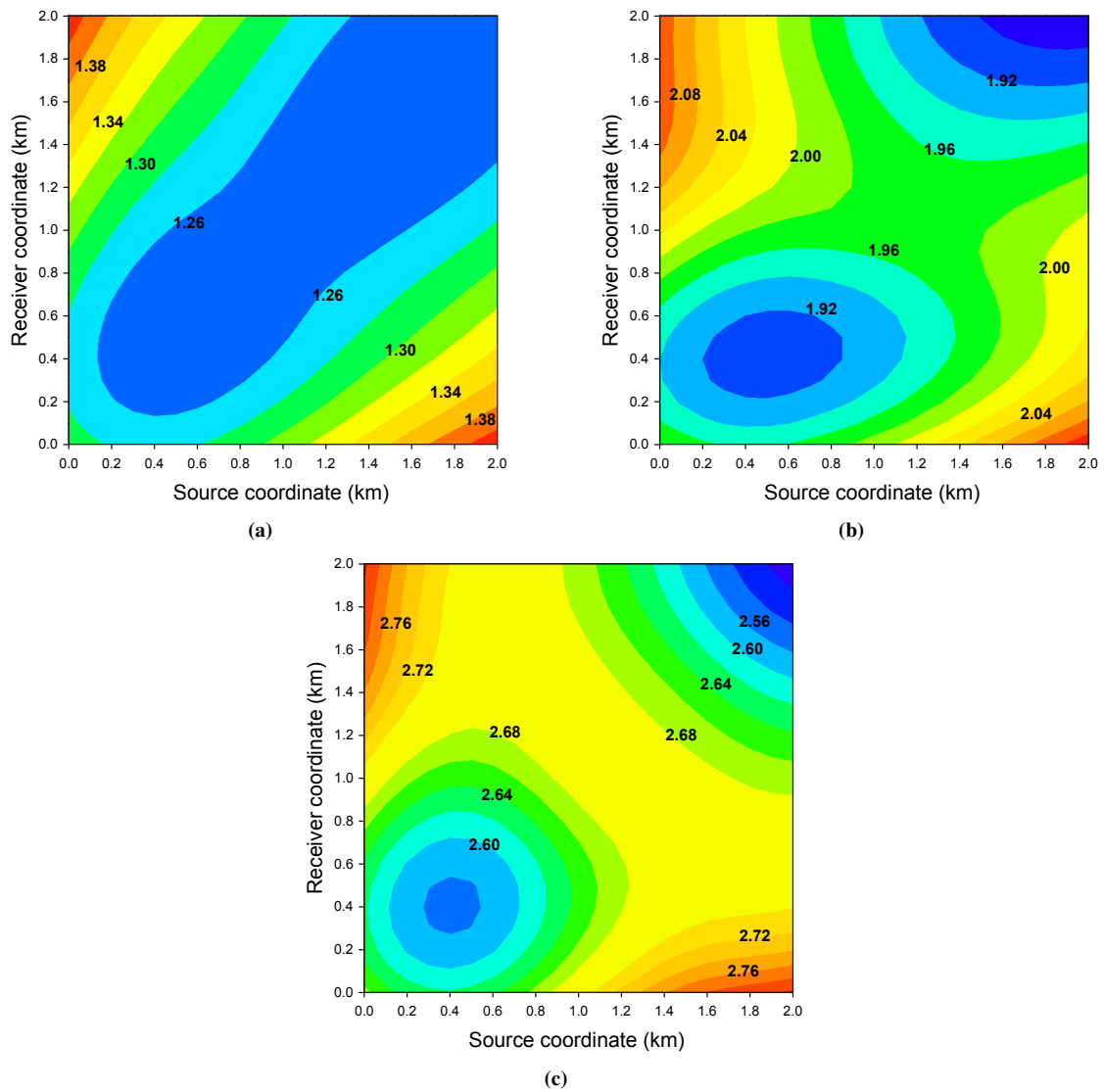


Figure 4: Simulated traveltime data for waves reflected at the lowermost model interface: (a) PP-wave, (b) PS-wave, and (c) SS-wave.

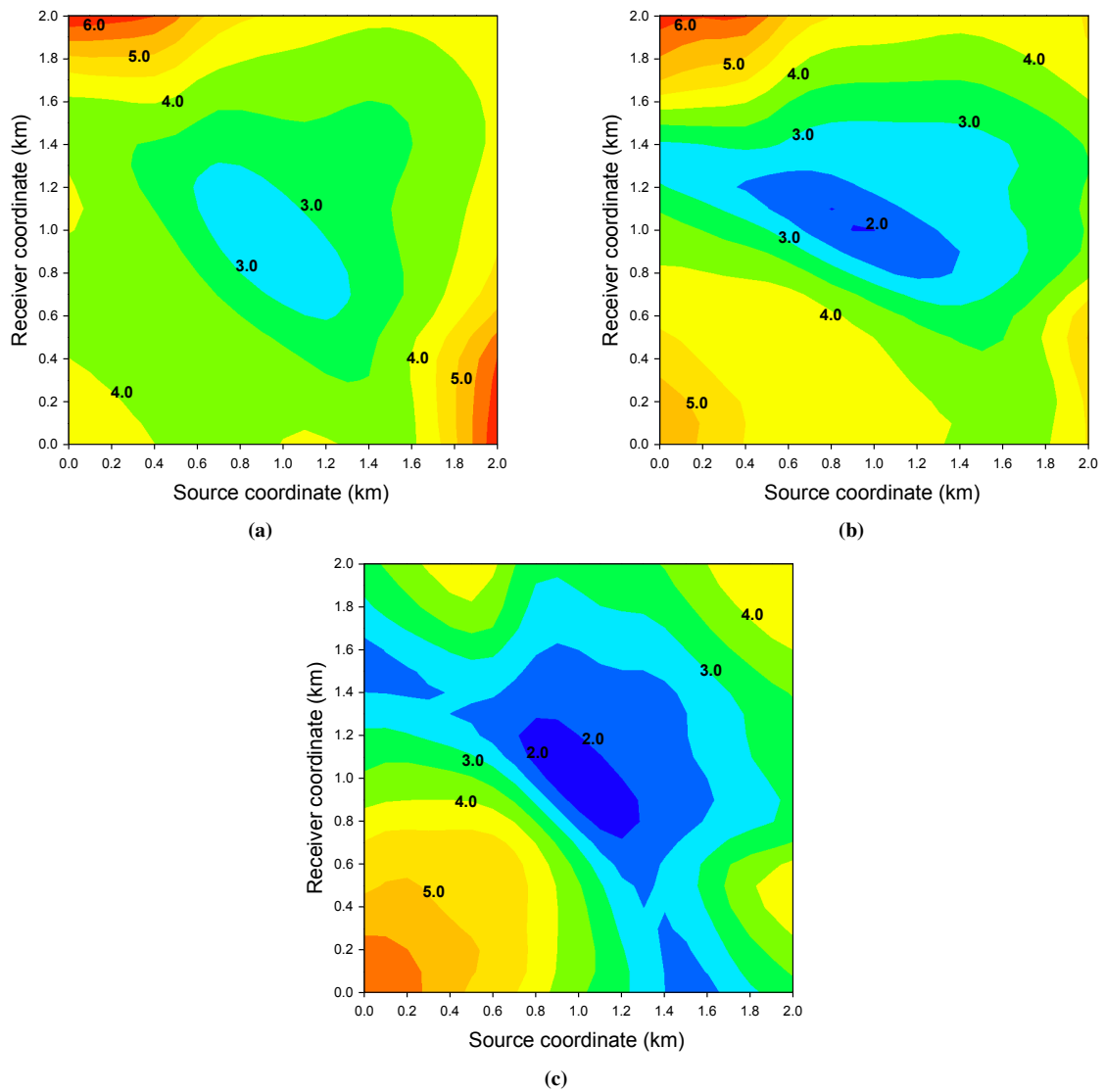


Figure 5: Simulated relative geometric spreading data for waves reflected at the lowermost model interface: (a) PP-wave, (b) PS-wave, and (c) SS-wave.

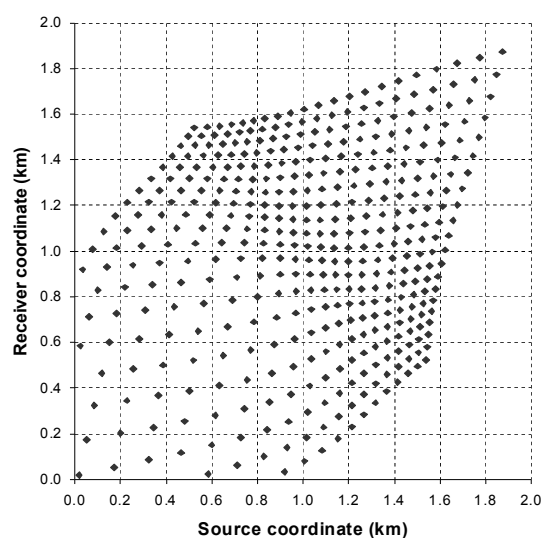


Figure 6: Reconstructed SS-wave source-receiver pairs for traveltimes and relative geometric spreading estimations.

observe that the traveltimes error introduced by the “PP+PS=SS” method, using noise-free input traveltimes, has a mean value of -0.002% and a standard deviation of 0.003% . Figure 8 shows results for the extended “PP+PS=SS” method. The (a) part shows the estimated SS-wave relative geometric spreading and is to be compared with Figure 5(a). The (b) part of Figure 8 shows the errors, which have a mean value of 0.1% and a standard deviation of 0.7% . We find the rise of the error level, compared to the errors of the estimated SS-wave traveltimes, quite natural in view of the fact that second derivatives of PP- and PS-wave traveltimes have been used to estimate the SS-wave relative geometric spreading.

CONCLUSIONS

For a given target reflector, the full surface-to-surface propagator matrix of an SS-wave can be obtained from the corresponding surface-to-surface propagator matrices of the PP- and PS-waves of the same reflector. This new result, which captures both the second-order derivatives of traveltimes of the SS-wave, extends the counterpart scheme of retrieving the SS-wave traveltimes and slope, known in the literature as the “PP+PS=SS” method. An interesting feature of the propagator matrix is that it allows for the computation of the relative geometric spreading, given that the elastic parameters determining the S-wave velocities along the acquisition surface are known. In this way, the geometric part of the amplitude of the SS-wave, namely the inverse relative geometric spreading factor, can be reconstructed. The reflection/transmission coefficients, which constitute the lithological (non-geometric) part of the amplitude, cannot be recovered from the amplitudes of the PP and PS waves.

The knowledge of the second-order derivatives of the SS traveltimes permits to determine, besides the relative geometric spreading, also the common-source and common-receiver traveltimes curvatures of the SS wave. In the same way as for PP waves, these quantities are very useful in setting up further constraints for the construction of a seismic velocity model by means of tomographic methods.

ACKNOWLEDGMENTS

We acknowledge support of the present work by VISTA, the *Research Council of Norway* via the ROSE project and NORSAR’s SIP project 181688/I30, the *National Council of Scientific and Technological Development (CNPq)*, Brazil and the sponsors of the *Wave Inversion Technology (WIT) Consortium*, Germany.

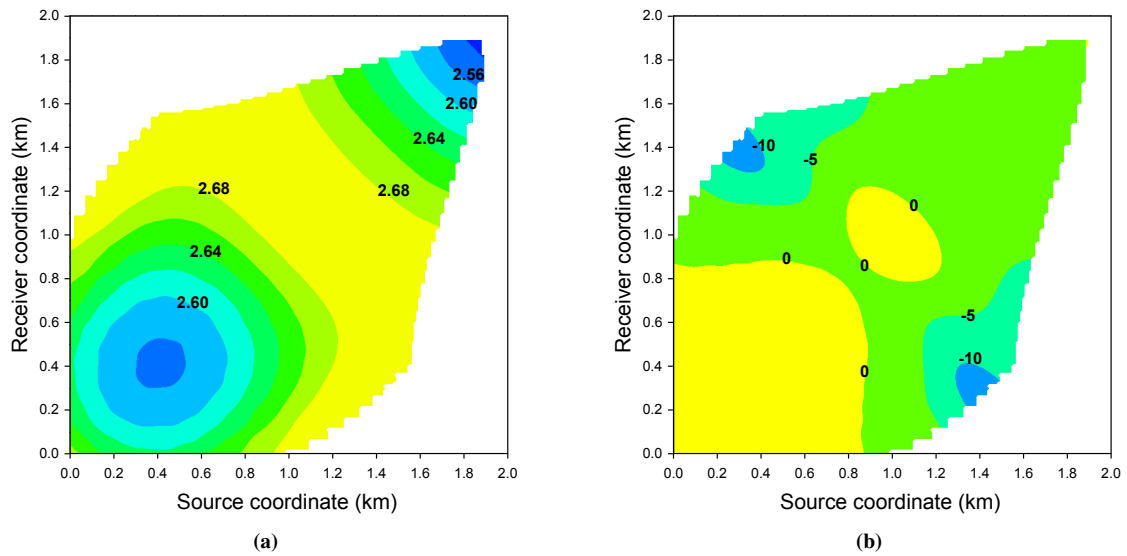


Figure 7: (a) Estimated SS-wave traveltime (s). (b) Error in estimated SS-wave traveltime (10^{-3} %). Mean value of the errors: -0.002 %. Standard deviation of the errors: 0.003 % .

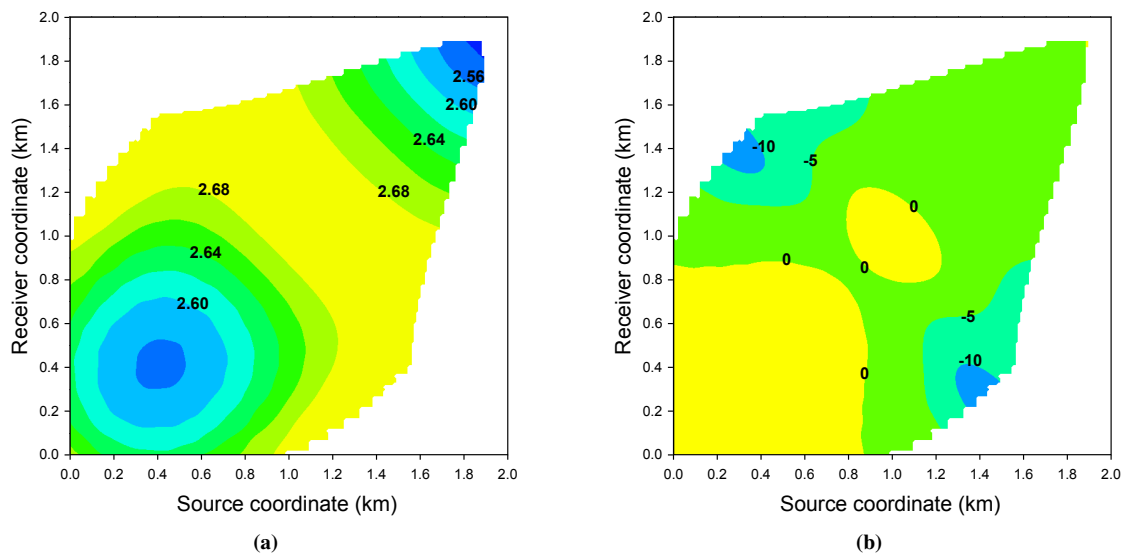


Figure 8: (a) Estimated SS-wave relative geometric spreading (km^2/s). (b) Error in estimated SS-wave relative geometric spreading (%). Mean value of the errors: 0.1 %. Standard deviation of the errors: 0.7 % .

REFERENCES

- Bortfeld, R. (1989). Geometrical ray theory: Rays and traveltimes in seismic systems (second-order approximations of the traveltimes). *Geophysics*, 54(3):342–349.
- Červený, V. (2001). *Seismic Ray Theory*, page 768. Cambridge University Press.
- Červený, V., Klimes, L., and Pšenčík, I. (1984). Paraxial ray approximation in the computation of seismic wavefields in inhomogeneous media. *Geophys. J. R. astr. Soc.*, 79:89–104.
- Chapman, C. H. (1994). Reflection/transmission reciprocities in anisotropic media. *Geophysical Journal International*, 116:498–501.
- Duveneck, E. (2004). 3D tomographic velocity model estimation with kinematic wavefield attributes. *Geophysical Prospecting*, 52:535–545.
- Foss, S.-K., Ursin, B., and de Hoop, M. (2005). Depth-consistent reflection tomography using PP and PS seismic data. *Geophysics*, 70(5):U51–U65.
- Gjøystdal, H., Reinhardsen, J. E., and Ursin, B. (1984). Traveltime and wavefront curvature calculations in three-dimensional inhomogeneous layered media with curved interfaces. *Geophysics*, 49(9):1466–1494.
- Grechka, V. and Tsvankin, I. (2002). PP + PS = SS. *Geophysics*, 67(6):1961–1971.
- Grechka, V., Tsvankin, I., Bakulin, A., Signer, C., and Hansen, J. (2002). Anisotropic inversion and imaging of PP and PS reflection data in the North Sea. *The Leading Edge*, 21(1):90–97.
- Hubral, P. (1983). Computing true amplitude reflections in a laterally inhomogeneous earth. *Geophysics*, 48(8):1051–1062.
- Iversen, E. (2006). Amplitude, Fresnel zone and NMO velocity for PP and SS normal-incidence reflections. *Geophysics*, 71(2):W1 – W14.
- Iversen, E. and Gjøystdal, H. (1984). Three-dimensional velocity inversion by use of kinematic and dynamic ray tracing. *Soc. of Expl. Geophys., 3rd Annual International Meeting*, pages 643–645.
- Stovas, A. and Ursin, B. (2003). Reflection and transmission responses of layered transversely isotropic viscoelastic media. *Geophysical Prospecting*, 51(5):447–477.
- Tessmer, G. and Behle, A. (1988). Common reflection point data stacking technique for converted waves. *Geophysical Prospecting*, 36:671–678.
- Thomsen, L. (1999). Converted-wave reflection seismology over inhomogeneous, anisotropic media. *Geophysics*, 64:678–690.
- Tsvankin, I. and Grechka, V. (2000). Two approaches to anisotropic velocity analysis of converted waves. *Soc. of Expl. Geophys., 70th Annual International Meeting*, pages 1193–1196.
- Tygel, M., Ursin, B., and Stovas, A. (2007). Convergence of traveltime power series for a layered VTI medium. *Geophysics*, 72(2):D21–D28.
- Ursin, B. (1982). Quadratic wavefront and traveltime approximations in inhomogeneous layered media with curved interfaces. *Geophysics*, 47(7):1012–1021.

APPENDIX A

Relative geometric spreading

The relative geometric spreading is given by Červený (2001)

$$\mathcal{L}(\mathbf{x}^r, \mathbf{x}^s) = |\det \mathbf{Q}_2(\mathbf{x}^r, \mathbf{x}^s)|^{1/2} = |\cos \varphi(\mathbf{x}^r) \cos \varphi(\mathbf{x}^s)|^{1/2} |\det \mathbf{B}(\mathbf{x}^r, \mathbf{x}^s)|^{1/2}, \quad (30)$$

where $\varphi(\mathbf{x}^r)$ and $\varphi(\mathbf{x}^s)$ are the phase angles of incidence and departure upon the acquisition surface at the source and receiver, respectively. These phase angles can not be readily extracted from the traveltimes observations, hence they need to be estimated under the assumption that the elastic parameters determining the phase velocities at the points \mathbf{x}^s and \mathbf{x}^r are known.

For simplicity and without loss of generality, assume that the acquisition surface is a plane $x_3 = 0$ and consider a projection (p_1, p_2) of the slowness vector (p_1, p_2, p_3) onto this surface. At the source and the receiver, the projections $(p_1, p_2)^s$ and $(p_1, p_2)^r$ are known from the corresponding slopes of the observed traveltimes function $T(x_1^r, x_2^r, x_1^s, x_2^s)$. The components p_3^s and p_3^r are, however, not known from this traveltimes function, but they are needed in order to obtain the phase angles in equation 30 for the relative geometric spreading. Along the acquisition surface, the component p_3 for a given wavetype is a function of the four variables (x_1, x_2, p_1, p_2) . Furthermore, the complexity of the computation of the component p_3 at the points \mathbf{x}^s or \mathbf{x}^r depends on the nature of the velocity model. For example, in the case of arbitrary anisotropy the component p_3 appears as a root of a sixth-order polynomial equation with coefficients constituted by all the 21 elastic moduli. For an isotropic medium, the component p_3 results from the relation

$$[p_3(x_1, x_2, p_1, p_2)]^2 = V^{-2}(x_1, x_2) - (p_1)^2 - (p_2)^2, \quad (31)$$

where V denotes the velocity of the P - or S -wave under consideration. Having computed $p_3(x_1, x_2, p_1, p_2)$, the corresponding cosine factor for the phase angle of incidence/departure required in equation 30 is given by

$$|\cos \varphi| = \frac{|p_3(x_1, x_2, p_1, p_2)|}{\sqrt{(p_1)^2 + (p_2)^2 + [p_3(x_1, x_2, p_1, p_2)]^2}}. \quad (32)$$

Applying equation 32 at the source as well as at the receiver and using in addition equation 20 in equation 30, one can compute the relative geometric spreading from the relation

$$\mathcal{L}(\mathbf{x}^r, \mathbf{x}^s) = |\det \mathbf{Q}_2(\mathbf{x}^r, \mathbf{x}^s)|^{1/2} = |\cos \varphi(\mathbf{x}^r) \cos \varphi(\mathbf{x}^s)|^{1/2} |\det \mathbf{M}^{rs}|^{-1/2}. \quad (33)$$

Finally, for a normal-incidence reflected wave at the point \mathbf{x} , we use equation 18 to obtain (Hubral, 1983)

$$\mathcal{L}(\mathbf{x}, \mathbf{x}) = 4 |\cos \varphi(\mathbf{x})| |\det(\mathbf{M}^{hh} - \mathbf{M}^{xx})|^{-1/2}. \quad (34)$$